

Silver Recovery from Radiographic Films Using an Electrochemical Reactor

P.A. Ramirez*, V.E. Reyes, M.A. Veloz

Área Académica de Ciencias de la Tierra y Materiales, Universidad Autónoma del Estado de Hidalgo. Carr. Pachuca-Tulancingo Km. 4.5, Mineral de la Reforma, Hidalgo, CP 42184, México.

*E-mail: pedroramirezortega@gmail.com

Received: 27 September 2011 / Accepted: 5 November 2011 / Published: 1 December 2011

Electrochemical studies were performed to recover silver from radiographic films on A304 stainless steel (A304 SS) and titanium (Ti) flat electrodes using a filter press-type electrochemical reactor (known as ER01-FP), as counter electrode was used a mesh-type DSA. Voltammetric studies were employed to find the current range under which silver reduction occurs for both electrodes. Using chronopotentiometric studies with controlled current, homogeneous deposits were obtained on the surface of the A304 SS and Ti electrodes. Scanning electron microscopy (SEM) and energy dispersive X-ray spectroscopy (EDS) studies corroborated the presence of silver on the A304 SS and Ti flat electrodes. Chronopotentiometric studies showed that the Ti flat electrode performed better for the recovery of silver because to a current of -150 mA during 210 minutes to a constant linear flow velocity of 15 Lmin⁻¹ was achieved 99.8% of silver recovery, with low energy consumption (E_s of 0.387 KWh/kg) and high current efficiency (ϕ^c of 99%). In addition, the silver concentration in the solution after the experiments was 1 ppm below environmental requirements for maximum recovery (5 ppm of silver in effluents). The ϕ^c and E_s values indicate the viability of a filter press-type electrochemical reactor (ER01-FP) for silver recovery from radiographic films.

Keywords: Silver recovery, radiographic films, electrochemical reactor, A304 SS, titanium

1. INTRODUCTION

Silver is an extremely important metal because of its various useful properties and its economic value. Silver is used in four major areas, including the industrial, photography, jewellery and coin sectors. Each year, the photography sector allocates approximately 45% of its silver to radiographic applications, which is discarded completely after it is used. Some technologies have attempted to recover the silver contained in these wastes. However, they have not met the environmental requirements for maximum recovery (less than 5 ppm of silver in effluents [1]. Today, electrochemical

and chemical methods are being used to recover the silver present in wastes generated by the photography sector. Among the most frequently used are ion exchange and silver plating in electrolytic units. Both processes have been broadly described in the literature [2-5], which shows the suitability of electrochemical processes due to their low cost of operation and high recovery values.

Several authors have studied the recovery of the silver present in effluents generated by the photography industry [6, 7]. However, in the case of solid wastes, information is lacking. Fundamental studies on this issue have shown that solutions such as nitric acid, cyanide, ammonia and potassium borohydride are suitable agents for dissolving silver found in solid wastes from the photography industry (radiographic films). They have also shown that it is convenient to use substrates such as stainless steel, titanium, silver and vitreous carbon as working electrodes to perform silver deposition [8-10]. Furthermore, fundamental studies of chemical speciation of a nitrate bath generated from the solid wastes of the radiography and photography industries have shown that the predominant species in the nitrate medium is Ag^+ and that hydrogen evolution does not interfere with its deposition [8].

A recent paper [11] showed that it is possible to electrochemically recover silver by electrodeposition on a DSA- O_2 mesh electrode surface from the waste products of an Ag(I)/Ag(II) redox system in a nitric acid medium used for mediated electrochemical processes. This study revealed that, at an optimised current density of 12 Adm^{-2} , 99% of silver Ag recovery efficiency was achieved with a high yield and a low energy consumption of 3.81 KWhkg^{-1} . However, the use of three-dimensional electrodes (DSA- O_2) introduces complexities into the removal of silver deposits.

At present, there are different types of electrochemical reactors that can be used for various processes, including Electrocell AB, FM01 and FM21-LC, which are used in laboratory studies, in pilot plants and on an industrial scale, respectively. These reactors increase mass transport through the use of turbulence promoters and deflectors. All of them have shown the ability to recover metals [12-16]. Therefore, this work examines silver recovery from radiographic films on a filter press-type electrochemical reactor (ER01-FP). These studies include cyclic voltammetric and chronopotentiometric investigations on A304 SS and Ti substrates using a filter press-type electrochemical reactor (ER01-FP) to determine the energetic conditions of current efficiency, energy consumption and Ag recovery efficiency when a deposit of silver is removed from the solid residue of radiographic film. Finally, the nature of the deposits on the surfaces of the A304 SS and Ti electrodes was verified using scanning electron microscopy (SEM) and energy dispersive x-ray spectroscopy (EDS).

2. MATERIALS AND METHODS

In this work, a filter press-type electrochemical reactor (ER01-FP) was used with a system of three electrodes (working, counter and reference). The capacity of the reactor was 280 mL. A304 SS and Ti (with a geometric area of 64.3 cm^2) were used as working electrodes, a saturated calomel electrode (SCE) was used as a reference, and a mesh-type DSA (titanium/ruthenium (IV) oxide) was used as the counter electrode.

The solutions used for the studies in this work included a nitric acid solution of 5%_{v/v} that was free of silver ions and a nitric acid solution of 5%_{v/v} with 250 g of radiographic film (initial concentration of 2100 ppm of Ag⁺), which are referred to below as the SRF solutions. Both solutions were prepared in the laboratory.

The electrochemical studies were carried out using a potentiostat-galvanostat PAR 263A connected to a KEPCO power source with a capacity of 10 A. The techniques used in the study utilised the software Power Suite®, provided by PAR.

SEM coupled with an EDS Jeol JSM-6300 was used to observe the morphology and the nature of the deposits obtained on the surface of the A304 SS and Ti electrodes. The images were obtained using secondary electrons at 30 kV.

3. RESULTS AND DISCUSSION

3.1. Voltammetric study

Figure 1 shows the voltammetric response at a scan rate of 25 mVs⁻¹ and a linear flow of 10 Lmin⁻¹ obtained from the solutions without (curve a) and with Ag⁺ ions (curve b) on the A304 SS and Ti substrates.

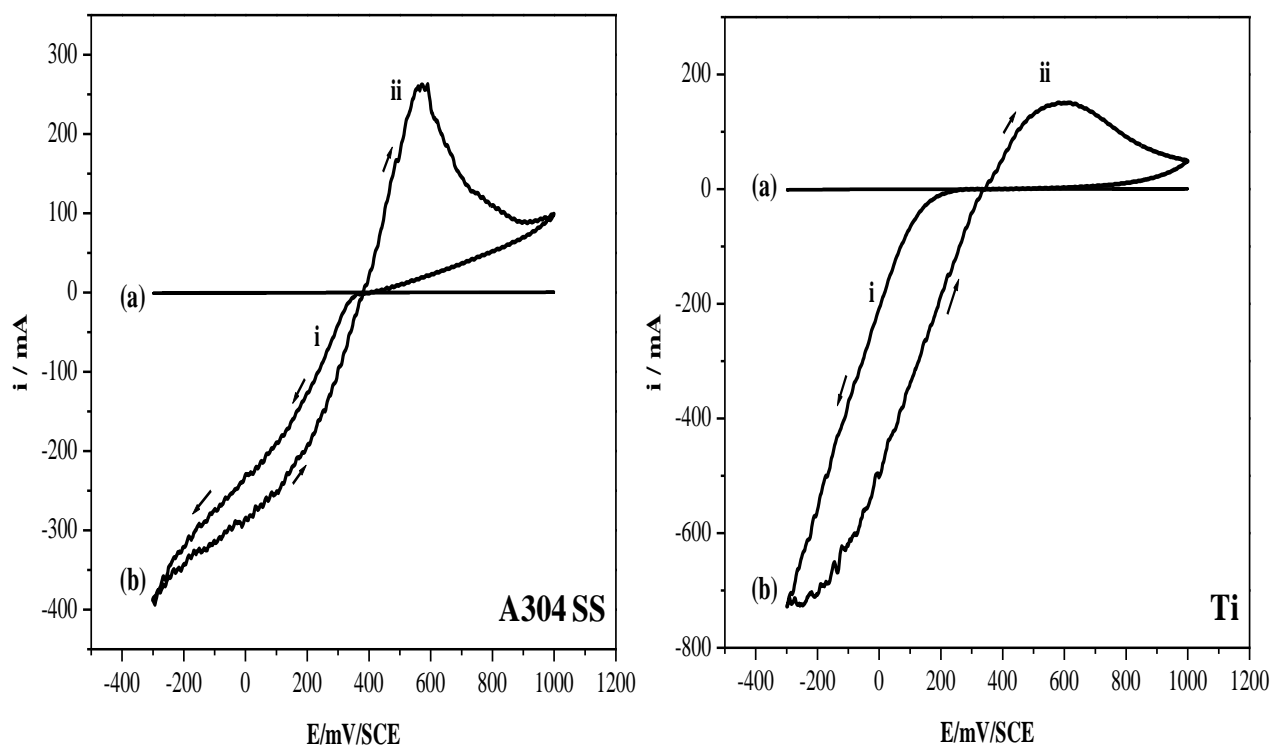


Figure 1. Voltammograms obtained from the SRF solution for the A304 SS electrode ($A=64.3 \text{ cm}^2$) and the Ti electrode ($A=64.3 \text{ cm}^2$). A scanning rate of 25 mV s^{-1} and a constant linear flow velocity of 10 Lmin^{-1} were used.

In the solution that contained no Ag^+ (curve a), there were not reduction or oxidation peaks corresponding to the reduction or oxidation of nitrate or substrates in the potential range studied for the A304 SS and Ti electrodes.

Figure 1 (curve b) shows that both electrodes (A304 and Ti) underwent two processes; the first was due to the reduction of silver (i) (approximately 300 to -300 mV/SCE for the A304 SS electrode and 150 to -300 mV/SCE for the Ti electrode), and the second corresponded to the oxidation processes of silver (ii) (approximately 400 to 800 mV/SCE for the A304 SS electrode and 350 to 900 mV/SCE for the Ti electrode).

Table 1 shows the over potential, the initial reduction current (where the reduction of Ag^+ present in the SRF solution occurs on the A304 SS and Ti electrodes) and the maximum current peak of silver oxidation. All of these parameters were obtained from an analysis of the voltammograms shown in Figure 1.

Table 1. Overpotential, initial reduction current and maximum current peak of silver oxidation at which the reduction of Ag^+ from the SRF solution on the A304 SS and Ti electrodes occurs.

Electrode	Over potential mV / SCE	Initial reduction current mA	Maximum current peak of silver oxidation mA
A304 SS	-79	-20	233
Titanium	-184.9	-10	150

Table 1 shows that both substrates have a clear response to the silver deposits. The A304 SS electrode presented a more defined response at the oxidation peak and a higher current, resulting in a greater amount of transformed mass.

The data indicate the current and potential values at which the reduction process of silver from the SRF solution on the A304 SS and Ti electrodes occurs. However, it was also necessary to perform chronopotentiometric studies to find a more narrow range for the current and to determine the optimum time for electrolysis when the silver is deposited onto both electrodes. Based on results obtained with the SRF solution, it was observed that, because of the increasing time required for electrolysis, more of the Ag^+ was transformed, which changed the surface of the electrodes and altered the energetic conditions of the potential and current at which the reduction of Ag^+ occurs.

Notably, in this work, all of the experiments used current values to facilitate the silver transfer because the use of a potential in any industrial process is much more complicated.

3.2. Chronopotentiometric study

Chronopotentiometric studies with a controlled current were carried out for an electrolysis time of 120 min and a linear flow velocity of 10 Lmin^{-1} . The current range used was obtained from the voltammetric studies. Notably, in this current range, the reduction of the medium did not significantly

affect the process of silver reduction. The current ranged from -40 to -125 mA for the A304 SS and Ti electrodes.

Figure 2 shows the galvanostatic transients on the A304 SS (Figure 2a) and Ti electrodes (Figure 2b). When the current acquired more cathodic values, the potential became more negative for all of the current ranges in both electrodes. However, over the entire current range, the potentials did not show any marked variation, indicating that the electroactive species of silver had not been exhausted due to the high concentration of Ag^+ in the SRF solution.

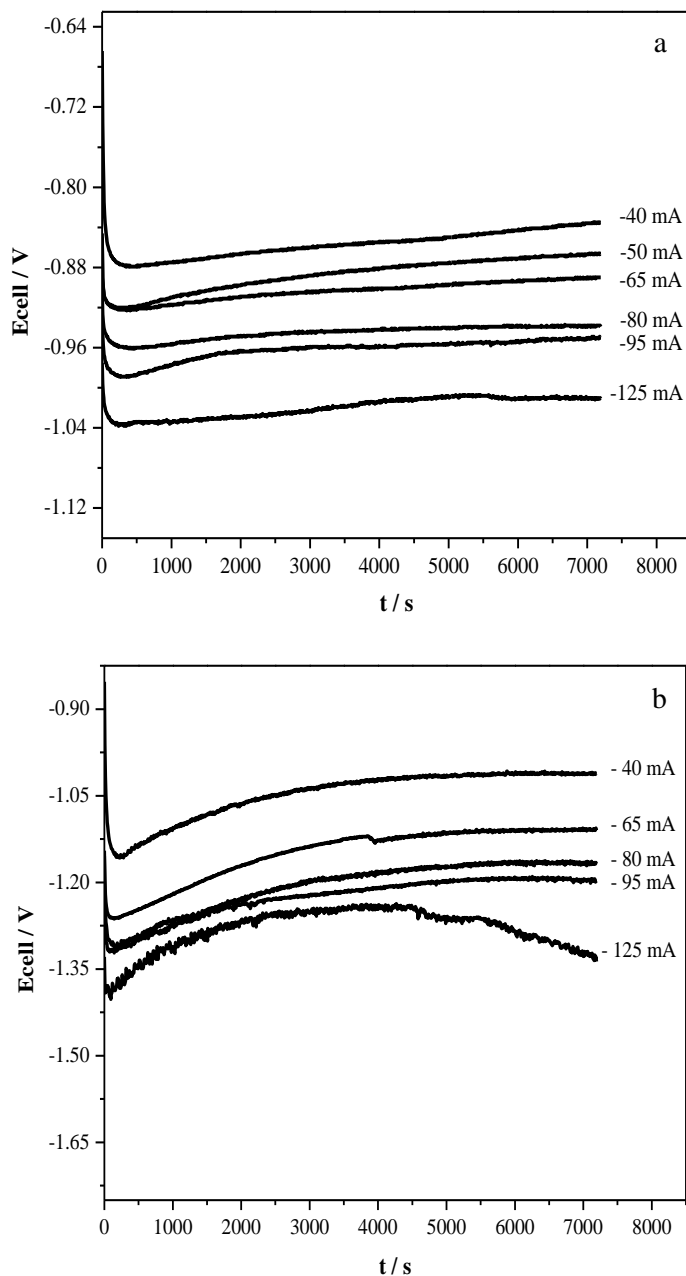


Figure 2. Chronopotentiograms obtained for the reduction of Ag^+ ions from the SRF solution for an electrolysis time of 120 min and a linear flow velocity of 10 Lmin^{-1} on a) the A304 SS electrode and b) the Ti electrode ($A=64.3 \text{ cm}^2$) for a current range of -40 to -125 mA.

Figure 3 shows the variation of the Ag^+ -normalised concentration with respect to the initial concentration, $C(t)/C(0)$, based on the electrolysis time using a current ranging from -40 to -125 mA on the A304 SS (Figure 3a) and Ti (Figure 3b) electrodes.

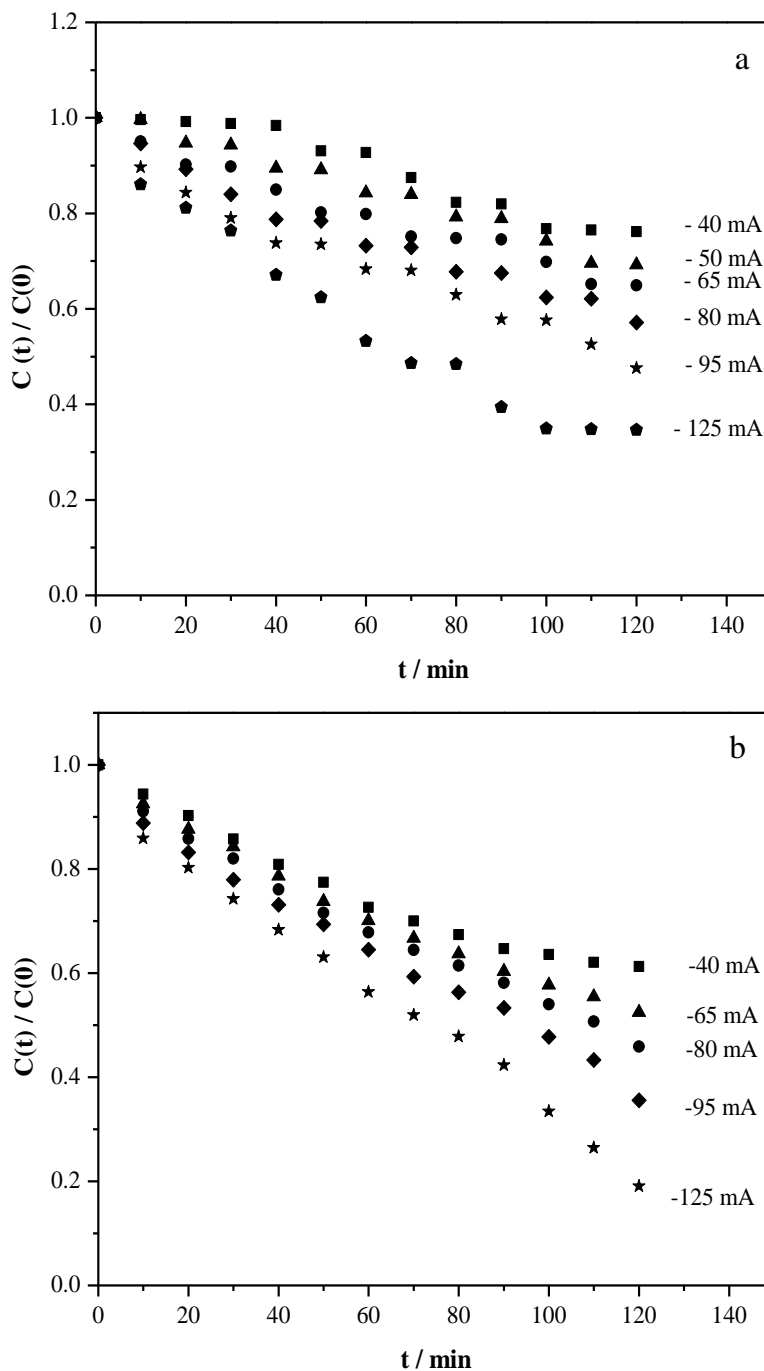


Figure 3. Variation of the Ag^+ -normalised concentrations of the SRF solution as a function of electrolysis time with imposed currents in the range of -40 to -125 mA for 120 min on a) the A304 SS electrode (area 64.3 cm^2) and b) the Ti electrode (area 64.3 cm^2) with a linear flow velocity of 10 Lmin^{-1} .

Figure 3 shows that the variation of the normalised concentration of Ag^+ decreased over the electrolysis time period for the six values of current imposed on the A304 SS electrode (Figure 3a) and the five values of current imposed on the Ti electrode (Figure 3b). In addition, in the current range imposed on both electrodes, there was also an increase in the silver deposit as the current became more cathodic.

The results of the chronopotentiometric study with controlled current indicate that the A304 SS electrode is suitable for silver recovery, but it is not the best choice because the silver recovery was only 67% at a current value of -125 mA. When using the same current value on the Ti electrode, silver recovery reached 80%. Therefore, the Ti electrode is the better choice for silver recovery.

3.3. Characterization of the deposits obtained on the A304 SS and Ti electrode surfaces

Figure 4 shows an image (200X) of the deposits obtained when imposing currents ranging from -40 to 125 mA on the A304 SS (Figure 4a) and Ti (Figure 4b) electrodes. Figure 4 also shows that there is a tendency for a greater amount of deposits to appear on the surface of the A304 SS and Ti electrodes as the current increases. The chronopotentiometric studies with a controlled current produced homogeneous deposits on the surfaces of both electrodes.

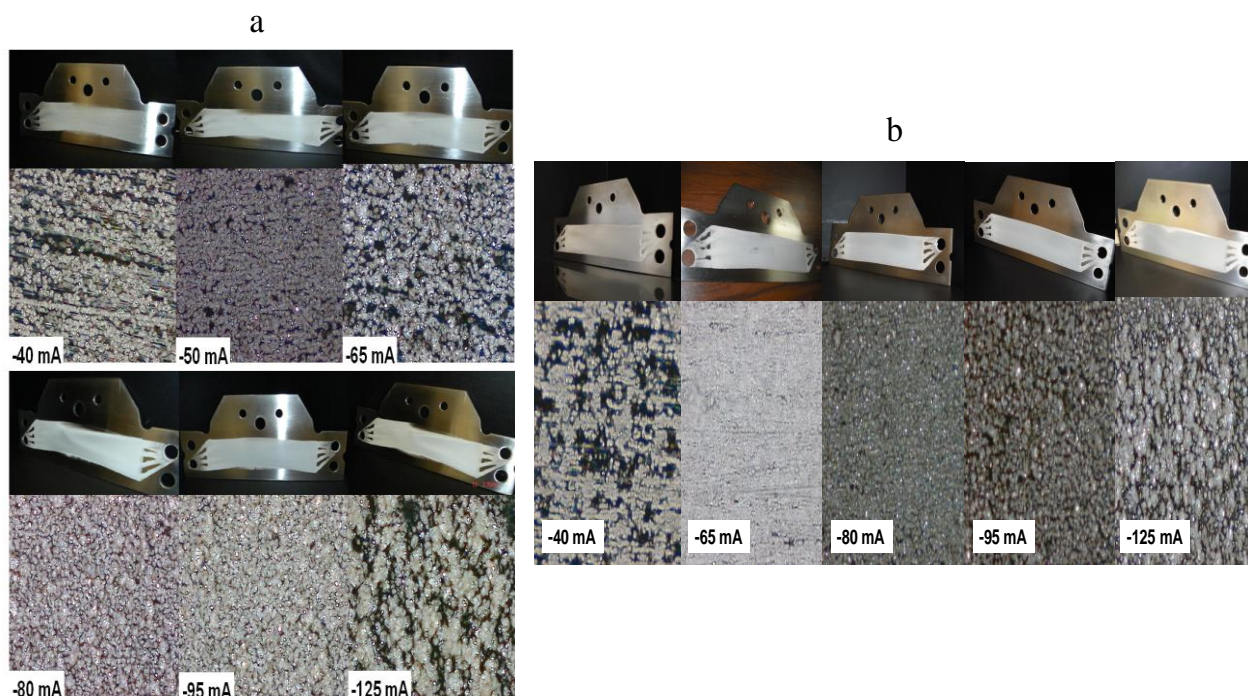


Figure 4. Deposits obtained on the surface of a) the A304 SS electrode (-40 to -125 mA) and b) the Ti electrode (-40 to -125 mA) at a linear flow velocity of 10 Lmin^{-1} over 120 min.

To verify that the deposit obtained on the surfaces of the A304 SS and Ti electrodes contained only metallic silver, scanning electron microscopy (SEM) and energy dispersive x-ray spectroscopy

(EDS) were performed on deposits that were extracted mechanically from the A304 and Ti electrode surfaces after an electrolysis time of 120 min. Figure 5 presents the image obtained by SEM of the products generated when imposing a current of -65 mA on the A304 SS (Figure 5a) and Ti (Figure 5b) electrodes for 120 min. The image was obtained using secondary electrons. It shows a massive metallic deposit from the products extracted from the A304 SS and Ti surfaces, which can be attributed to the silver present in the solution. In addition, the EDS confirmed that the deposits obtained on the A304 SS and Ti electrodes were silver.

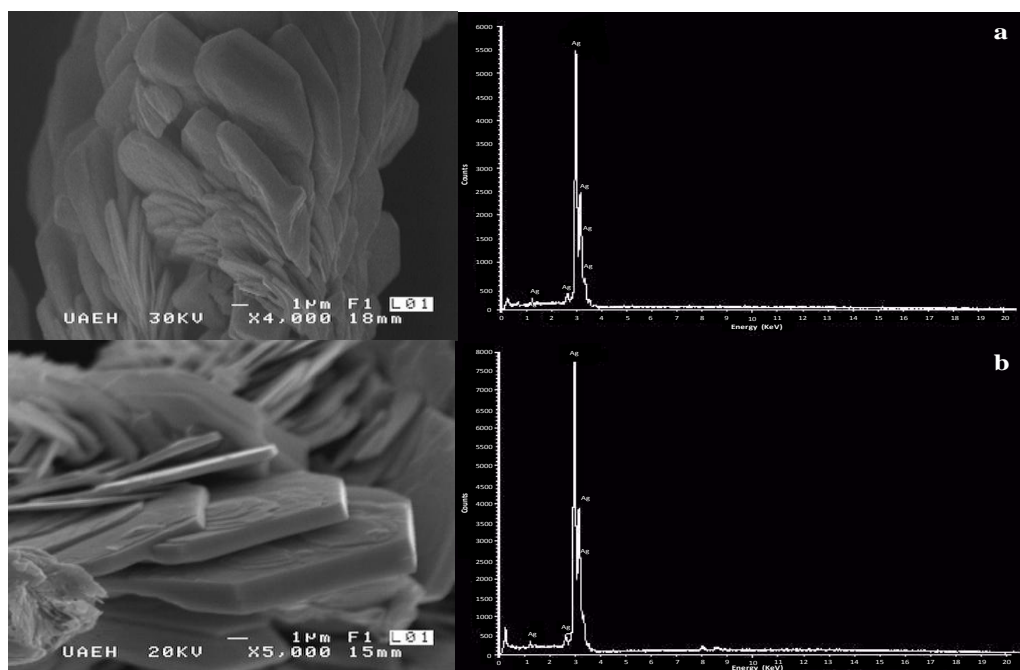


Figure 5. Scanning electron microscopy (SEM) images and EDS results of deposits obtained after 120 min of electrolysis in the SRF solution using a current of -65 mA on a) the A304 SS electrode and b) the Ti electrode. The images of the deposits were obtained using secondary electrons.

To investigate the effect of the hydrodynamic conditions on the electrochemical deposition of the silver on the surface of the Ti electrode, a chronopotentiometric study at a controlled current was carried out by varying the flow velocity of the SRF solution through the reactor. The linear flow velocities ranged from 7.5 to 15 Lmin⁻¹.

3.4. Chronopotentiometric studies with different flow velocities

Chronopotentiometric studies with different flow velocities were performed for an electrolysis time of 120 minutes with a constant current of -65 mA in all experiments. This current was selected to avoid hydrogen evolution.

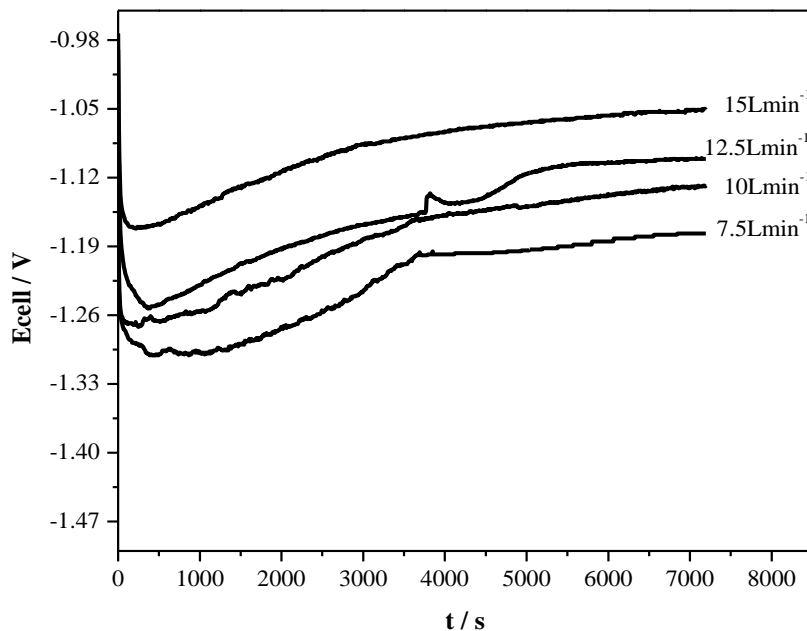


Figure 6. Chronopotentiograms obtained for the reduction of Ag⁺ ions from the SRF solution for 120 min of electrolysis with a constant current of -65 mA on the Ti electrode (area: 64.3cm²) and linear flow velocities ranging from 7.5 to 15 Lmin⁻¹.

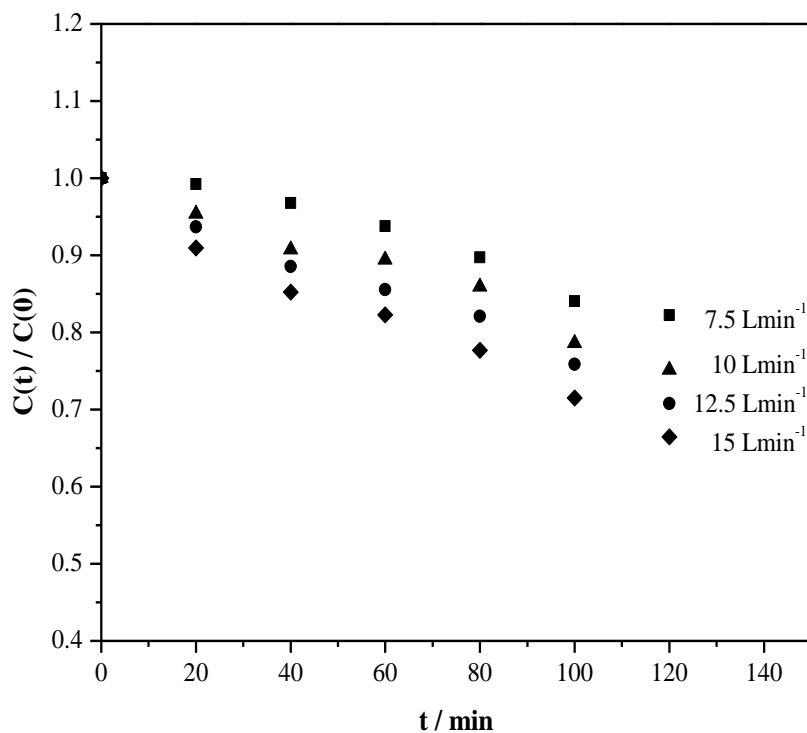


Figure 7. Variation of the Ag⁺-normalised concentrations of the SRF solution as a function of electrolysis time with an imposed current of -65 mA on the Ti electrode (area: 64.3c m²) with linear flow velocities ranging from 7.5 to 15 Lmin⁻¹.

Figure 6 shows the galvanostatic transients obtained on the Ti electrode. The studies conducted with linear flow velocities ranging from 7.5 to 15 Lmin⁻¹ showed that, as the flow velocity increased, the potential values became less negative. Conversely, it was observed that, in each transient, the potential became less negative as the electrolysis time increased. This behaviour indicates that the silver nucleation on the surface of the Ti electrode results in less energy that is required to deposit the silver. Furthermore, the hydrodynamic conditions caused a greater amount of Ag⁺ to collect at the interface.

Figure 7 shows the variation of the Ag⁺-normalised concentration with respect to the initial concentration, C(t)/C(0), based on the electrolysis time with imposed flow velocities ranging from 7.5 to 15 Lmin⁻¹ on the Ti electrode. This figure shows that the variation of the normalised concentration of Ag⁺ decreased with respect to the electrolysis time for the four flow velocities imposed on the Ti electrode. In addition, the recovery of silver increased as the flow velocity increased, and the silver recovery reached 34% at a linear flow velocity of 15 Lmin⁻¹.

3.5. Characterization of the deposits obtained on the surface of the Ti electrode

Figure 8 shows the deposits obtained on the surfaces of the Ti (200X) electrode when imposing linear flow velocities ranging from 7.5 to 15 Lmin⁻¹. The figure indicates that the amount of the deposit on the surface of the Ti electrode increased as the flow velocity increased. As was found in the chronopotentiometric studies with a controlled current, homogeneous deposits appeared on the Ti electrode under all of the flow velocities used.

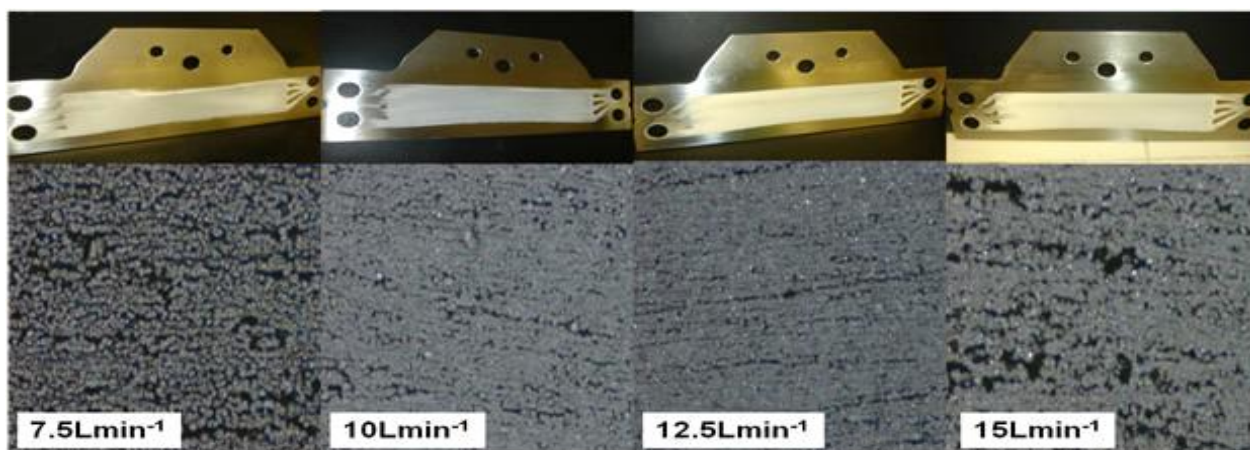


Figure 8. Deposits obtained on the surface of the Ti electrode (area: 64.3 cm²) for linear flow velocities ranging from 7.5 to 15 Lmin⁻¹.

Figure 9 shows an SEM image of the deposits mechanically removed from the surface of Ti electrode under a linear flow velocity of 7.5 Lmin⁻¹ (Figure 9a) and 15 Lmin⁻¹ (Figure 9b) for 120 min. The images were obtained using secondary electrons and show the morphology of the silver deposit on the Ti electrode surface. These deposits were analysed by EDS (Figure 9), which revealed that the

deposits were metallic silver. It's important to mention that all the deposits obtained on titanium and A304 SS flat electrodes were easily removed using a Teflon spatula, avoid other more complex processes such as those used when the deposit is made on three-dimensional or mesh electrodes [11].

Based on these results, and with the aim of exhausting the Ag^+ that was present in the SRF solution, a chronopotentiometric study of a controlled current was performed over 210 min with a constant current of -150 mA and a linear flow velocity of 15 Lmin^{-1} .

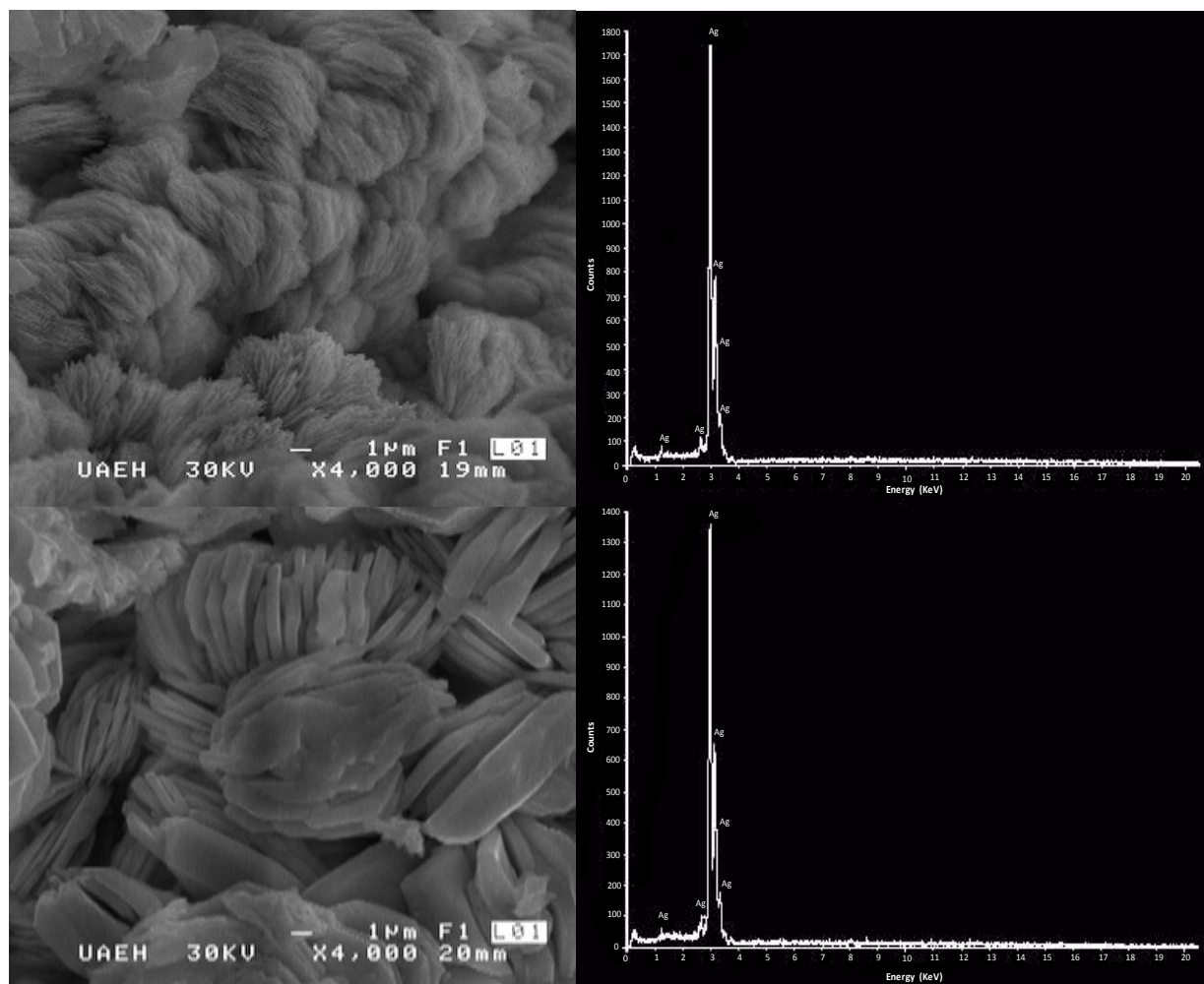


Figure 9. Scanning electron microscopy (SEM) images and EDS results of deposits obtained after 120 min of electrolysis in the SRF solution on the Ti electrode with an imposed current of -65 mA and linear flow velocities of 7.5 and 15 Lmin^{-1} . The images of the deposits were obtained using secondary electrons.

Figure 10 shows the variation of the Ag^+ -normalised concentration with respect to the initial concentration, $C(t)/C(0)$, based on the electrolysis time with an imposed current of -150 mA and a constant linear flow velocity of 15 Lmin^{-1} on the Ti electrode for an electrolysis time of 210 min. The variation of the normalised concentration of Ag^+ diminished over time. In addition, after 210 min, Ag recovery reached 99.8%. It's important to mention that the silver concentration in solution after of the

studies was 1ppm this concentration is below environmental requirements for silver maximum recovery (5 ppm of silver in effluents) [1]. Figure 11 shows the deposit obtained on the Ti electrode (200X) for a current of -150 mA for 210 min. A homogeneous deposit was present on the Ti electrode surface and showed the same morphology as the silver deposits obtained in the chronopotentiometric studies conducted at different flow velocities.

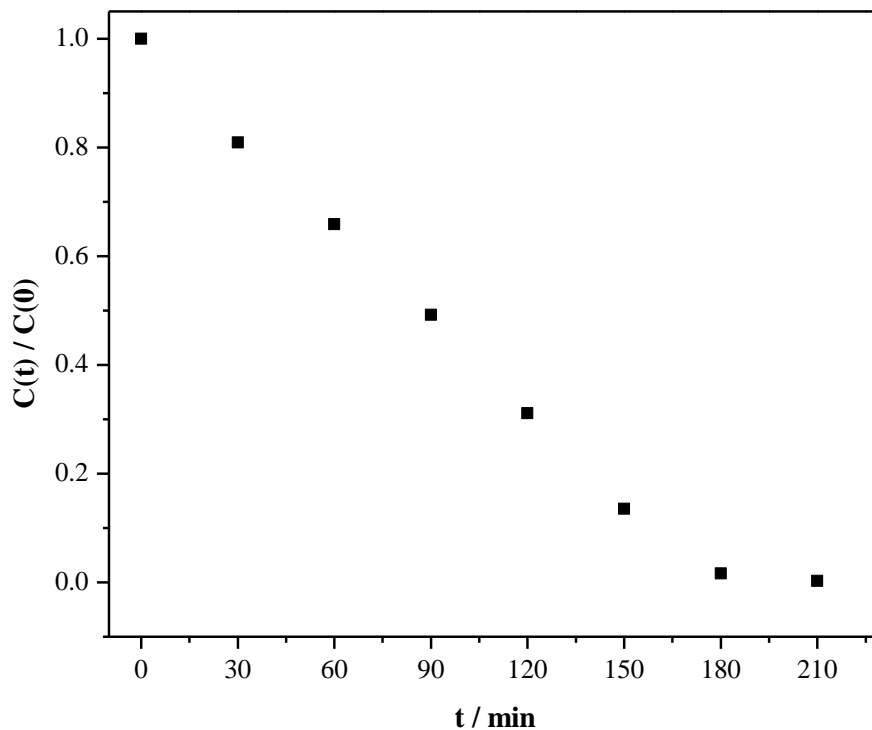


Figure 10. Variation of the Ag^+ -normalised concentrations from the SRF solution as a function of the electrolysis time (210 min) with an imposed current of -150 mA on the Ti electrode (area: 64.3cm^2) and a linear flow velocity of 15Lmin^{-1} .

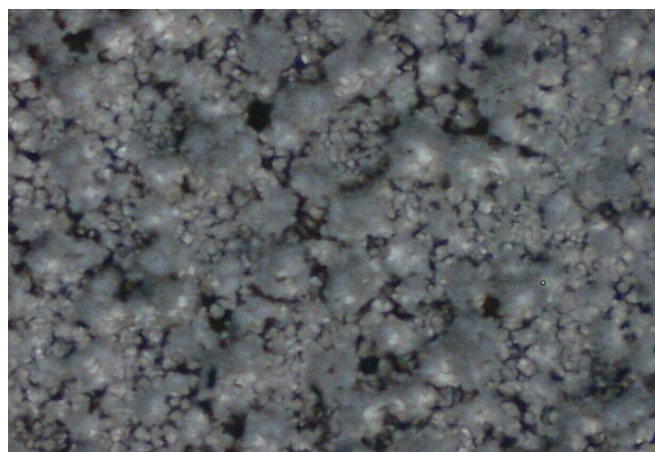


Figure 11. Deposits obtained on the surface of the Ti electrode (200X) when imposing a current of -150 mA with a linear flow velocity of 15Lmin^{-1} for 210 min.

3.6. Current efficiency ϕ^e and energy consumption E_s

$$\phi^e = \frac{W_j}{W_{TOTAL}} \quad (Eq. 1)$$

$$E_s = -\frac{nFE_{cell}}{\phi^e} \quad (Eq. 2)$$

where ϕ^e is the current efficiency, W_j is the weight of metal j deposited, W_{total} is the weight of the deposit that should be obtained by imposing a current over a certain amount of time, E_s is the energy consumption, n is the number of electrons transferred, F is the Faraday constant, and E_{cell} is the cell voltage.

The current efficiency ϕ^e (Eq. 1) and energy consumption E_s values (Eq. 2) were calculated by weighing the silver powder obtained on the Ti electrode surface W_j after imposing a constant current of -150 mA during 210 minutes to a constant flow velocity of $L\text{min}^{-1}$ and comparing this weight with the those from the currents used for the deposition W_{total} [17,18]

The current efficiency and energy consumption E_s values (Eq. 2) were calculated by weighing the silver powder obtained on the Ti electrode under a constant current of -150 mA and comparing this weight with the those from the currents used for the deposition w_{total} [17,18]. The efficiency value was 99%, with an energy consumption of 0.387 KWhkg^{-1} . These high current efficiency and low energy consumption values demonstrate the excellent performance of the electrochemical reactor ER01-FP for the recovery of silver from an SRF solution, as compared to others discussed in the literature [11].

4. CONCLUSIONS

Voltammetric studies of SRF solutions in an electrochemical reactor (ER01-FP) showed that the reduction and oxidation processes observed on A304 SS and Ti electrodes occurred due to the deposition and dissolution of silver and did not arise from other ionic species in the SRF solution.

Chronopotentiometric studies with a controlled current produced homogeneous deposits on the surfaces of the A304 SS and Ti electrodes. These deposits were analysed by EDS and were found to be metallic silver. In addition, this study found a more precise current range under which the deposition of silver takes place. Chronopotentiometric studies performed at different linear flow velocities showed that the recovery of silver increased with increasing flow velocity. The Ti dimensional electrode performed better for silver recovery.

For a current of -150 mA and an electrolysis time of 210 min, silver recovery reached 99.8% on Ti flat electrode. The high current efficiency (99%) and low energy consumption (0.387 KWhkg^{-1}) values at a constant current value of -150 mA indicate that the filter press-type electrochemical reactor (ER01-FP) used in this study is an excellent option for the recovery of silver from SRF solutions.

ACKNOWLEDGMENTS

The authors would like to express their gratitude to Fomix Hidalgo (project number 97597) and CONACyT (project number 90821) for their economic support. Pedro A. Ramirez Ortega thanks CONACyT for his Ph.D. scholarship.

References

1. NOM-CCA-017-ECOL/1993., *Límites máximos permisibles de contaminantes en las descargas de aguas residuales a cuerpos receptores provenientes de la industria de acabados metálicos*, Norma Oficial Mexicana (1993).
2. K. Guenter, *review of the methods chemical labor Betr.*, 32 (1981) 40-48.
3. D. E. Kimbrough et al., *J. of solid waste Technology and Management.*, 23 (1996) 197-207.
4. M. T. Oropeza, C. Ponce de León and I. González, *Ingeniería Electroquímica Principios y Aplicaciones*, Ed. Sociedad Mexicana de Electroquímica: D.F., México (1995).
5. Environment Information from Kodak, Eastman Kodak Company, (1999) J-212.
6. M. E. Chatelut et al., *Hydromet.* 54 (2000) 79-90.
7. A.A. Melo L. *Estudios electroquímicos preliminares en un reactor tipo prensa para la recuperación de Ag proveniente de los efluentes de la industria Fotográfica y Radiográfica*, Bachelor degree Thesis, Universidad Autónoma del Estado de Hidalgo, México (2006).
8. P. A. Ramírez O., *Estudio electroquímico preliminar para depositar Ag proveniente de los desechos sólidos de la industria fotográfica y radiográfica*, Bachelor degree Thesis, Universidad Autónoma del Estado de Hidalgo, México (2005).
9. H. Zhouxiang et al., *Hydromet.* 92 (2008) 148-151.
10. S. Syed et al., *Hydromet.* 63 (2002) 277-280.
11. T. Raju, S. Joon C., and I. Shik M., *Korean J. Chem. Eng.*, 26(4) (2009) 1053-1057.
12. F. C. Walsh and D. Robinson, *Chemical Technology Europe*, (1995) pp. 16.
13. D. Pletcher and F. C. Walsh, *Industrial Electrochemistry*, 2nd Edition, Chapman & Hall: London (1990).
14. F. C. Walsh, *A First Course in Electrochemical Engineering*, The Electrochemical Consultancy: England (1993).
15. J. Arthur and J. Forrest, *J. Desal.*, 149 (1889) 375.
16. J. Gutiérrez and L. Horita, *Recuperación de Plata*, Bachelor degree Thesis, Universidad Autónoma Metropolitana-Iztapalapa, México (2003).
17. M. Schlesinger and M. Paunovic, *Modern Electroplating, fourth edition*, While Interscience Publication: United State of America (2000).
18. A.J. Bard and L. R. Faulkner, *Electrochemical methods: fundamentals and applications*, 2nd Edition, Wiley: United State of America (2000).